Effects of AlN nucleation layer thickness on crystal quality of AlN grown by plasma-assisted molecular beam epitaxy*

Ren Fan(任 凡), Hao Zhi-Biao(郝智彪)†, Hu Jian-Nan(胡健楠), Zhang Chen(张 辰), and Luo Yi(罗 毅)

Tsinghua National Laboratory for Information Science and Technology, State Key Laboratory on Integrated Optoelectronics, Department of Electronic Engineering, Tsinghua University, Beijing 100084, *China*

(Received 24 March 2010; revised manuscript received 11 May 2010)

In this paper, the effects of thickness of AlN nucleation layer grown at high temperature on AlN epi-layer crystalline quality are investigated. Crack-free AlN samples with various nucleation thicknesses are grown on sapphire substrates by plasma-assisted molecular beam epitaxy. The AlN crystalline quality is analysed by transmission electron microscope and x-ray diffraction (XRD) rocking curves in both (002) and (102) planes. The surface profiles of nucleation layer with different thicknesses after *in-situ* annealing are also analysed by atomic force microscope. A critical nucleation thickness for realising high quality AlN films is found. When the nucleation thickness is above a certain value, the (102) XRD full width at half maximum (FWHM) of AlN bulk increases with nucleation thickness increasing, whereas the (002) XRD FWHM shows an opposite trend. These phenomena can be attributed to the characteristics of nucleation islands and the evolution of crystal grains during AlN main layer growth.

Keywords: aluminum nitride, plasma-assisted molecular beam epitaxy, nucleation layer
PACC: 6855, 7280E, 6110M, 6170J

1. Introduction

AlN has a very wide bandgap of 6.2 eV, high thermal conductivity, high chemical and thermal stability, therefore it is a potential semiconductor material for applications in microelectronic and UV optoelectronic devices, including high electron mobility transistors (HEMTs), UV light emitting diodes (LEDs) and solar blind detectors.[1−3] AlN thin film could also be used as an epitaxy template to improve the crystalline quality of GaN-based epi-layer.[4,5] However, because of the large lattice mismatch between AlN and sapphire as well as poor Al adatom migration ability, high-quality AlN growth on sapphire substrate is more difficult than GaN either by metal-organic vapour phase epitaxy (MOVPE) or molecular beam epitaxy (MBE).

Similar to GaN growth procedure, the initial growth stage plays a very important role in AlN epitaxy. For MOVPE technology, the effects of initial stage on the surface morphology and structure properties of AlN epi-layers were studied.[6,7] For MBE growth, a high-temperature AlN nucleation layer is usually adopted to achieve Al-polarity. Fälth *et al.*[8] reported a flat AlN surface with a root-mean-square (RMS) roughness of 0.9 nm using a nucleation layer grown under N-rich condition combined with a V/III ratio of 1 for AlN main layer. However, the influence of the thickness of AlN nucleation layer on crystalline quality has not been studied in detail. In the present work, AlN materials with high-temperature nucleation layers of different thicknesses are grown on sapphire substrates by plasma-assisted MBE (PAMBE), and the effects of nucleation layer thickness on AlN crystalline quality are discussed.

2. Experiment

All of the samples were grown on (0001) sapphire substrates by an SVTA PAMBE system with a radio-frequency (RF) plasma nitrogen source. A reflection high energy electron diffraction (RHEED) sys-

*Project supported by the National Natural Science Foundation of China (Grant Nos. 60536020 and 60723002), the National Basic Research Program of China (Grant Nos. 2006CB302800 and 2006CB921106), the National High Technology Research and Development Program for Advanced Materials of China (Grant No. 2006AA03A105), and the Major Project of Beijing Municipal Science and Technology Commission, China (Grant No. D0404003040321).
†Corresponding author. E-mail: zbhao@tsinghua.edu.cn
© 2010 Chinese Physical Society and IOP Publishing Ltd

tem was equipped for *in-situ* monitoring the surface atom construction. Additionally, an IS4000 system was mounted normally facing the substrate to record substrate temperature and optical reflectivity. The growth rate of epi-layer can be calculated from the oscillation curve of surface optical reflectivity. The Al and N fluxes are evaluated by measuring growth rates,[9] and the V/III ratio can be conveniently determined. The surface morphologies of the as-grown samples were characterised by atomic force microscope (AFM). The AlN crystalline qualities were analysed with x-ray diffraction (XRD) in both (002) and (102) planes. The screw and edge threading dislocations (TDs) in AlN epi-layers were observed by transmission electron microscope (TEM).

The substrates were outgassed for 1 h at 500 °C before growth. Then the nitridation process was carried out at a substrate temperature of 780 °C with an RF power and a nitrogen gas flow of 400 W and 3 sccm, respectively. The AlN nucleation layer was grown on the fully nitridated surfaces at 760 °C with a V/III ratio of 1.04, followed by an *in-situ* annealing. Then 1-μm-thick AlN main layers were grown with a V/III ratio of 0.95 at a substrate temperature of 820 °C. The growth rates of nucleation and main layers, determined by growing thicker layers under corresponding conditions, are about 500 and 490 nm/h, respectively. Four AlN samples (A1, B1, C1 and D1) were grown using the same procedures, except for using different nominal nucleation layer thicknesses of 6.5 nm, 12.5 nm, 25 nm and 50 nm, respectively. In order to investigate the characteristics of the nucleation layers, another set of samples (A2, B2, C2 and D2) was prepared under the same conditions as those of the above four samples, just except for not growing AlN main layers.

3. Results and discussion

Before the nitridation, a streaky RHEED pattern of sapphire surface was obtained. After the nitridation, the RHEED pattern transformed into AlN characteristic, indicating that the sapphire surface had fully converted into AlN structure of a few atomic layers in thickness. As soon as the nucleation layer growth started, the streaky RHEED pattern immediately changed into a spotty one. This phenomenon reflects that AlN islands formed at the initial growth stage due to a large lattice mismatch of 13% between AlN and sapphire. During the nucleation annealing, unlike GaN nucleation, there was no obvious change observed either in RHEED pattern or in surface optical reflectivity. This implies that the *in-situ* high-temperature annealing process does not induce decomposition or recrystallisation even in high vacuum environment, resulting from the fact that Al–N bond is stronger than Ga–N bond.[10]

During the growth of the AlN main layer, the spotty RHEED pattern gradually transformed back to a streaky one in 20–25 min. The typical 1×1 RHEED pattern along the AlN [11$\bar{2}$0] direction is shown in Fig. 1. Clear 0, ±1 order diffraction streaks and Kikuchi lines can be observed, indicating that highly ordered periodic structures have been obtained for all AlN samples. These streaky RHEED patterns were well maintained to the end of the growth, and no reconstruction occurred. Moreover, the surface optical reflectivity showed a steady periodic oscillation.

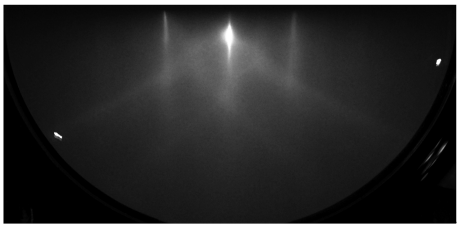


Fig. 1. Typical RHEED image along the AlN [11$\bar{2}$0] direction after growth.

The XRD rocking curves in (002) and (102) planes of the AlN samples are shown in Fig. 2. The screw and edge TD densities of each bulk material sample can be estimated by fitting XRD full width at half maximums (FWHMs) in a serial of different planes.[11−16] The XRD ω-scan FWHMs, surface RMS roughness results and estimated TD densities of the AlN samples are listed in Table 1. Figure 3 shows the typical (Sample C1) bight-field cross-sectional TEM images under two different diffraction conditions with $g = [0002]$ in Fig. 3(a) and $g = [10\bar{1}0]$ in Fig. 3(b), which reveal screw and edge TDs, respectively. The screw and edge TD densities are determined from TEM images in a larger scan area to be 5×10^7 cm^{-2} and 1.2×10^{10} cm^{-2}, respectively. These results are in good agreement with the estimations from XRD measurements, which can be a good evaluation on the crystalline quality of AlN epi-layer. For sample B1 with a 12.5 nm nucleation layer, a (102) XRD FWHM as narrow as 851 arcsec has been obtained, which, to the authors' knowledge, is one of the best results reported for AlN grown by MBE so far.

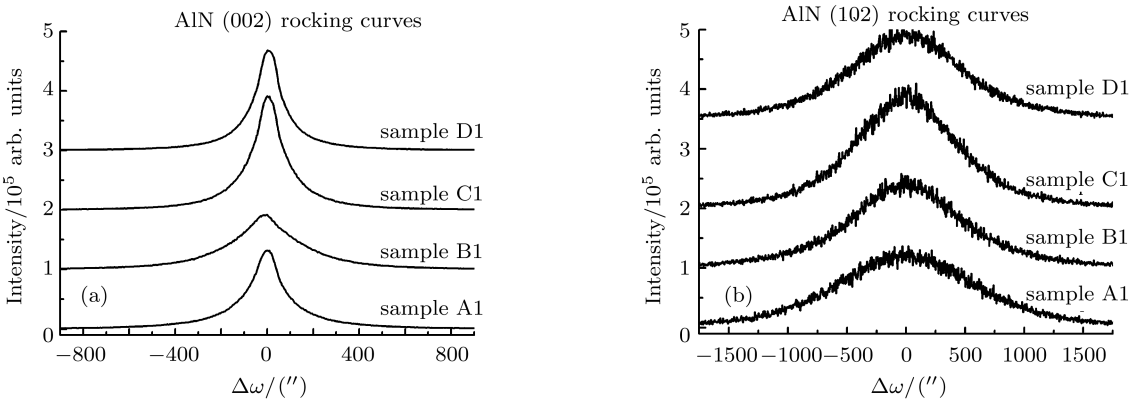


Fig. 2. XRD rocking curves of samples A1, B1, C1 and D1 in (002) plane (a) and (102) plane (b).

Table 1. XRD, AFM results and estimated TD densities of the AlN samples with different nucleation layer thicknesses.

sample	nucleation thickness/nm	XRD FWHM/(″) (002) plane	XRD FWHM/(″) (102) plane	5×5 μm^2 RMS roughness/nm	screw TD density /×10^7 cm^{-2}	Edge TD density /×10^9 cm^{-2}
A1	6.5	165	1197	0.4	5.9	17.1
B1	12.5	292	851	10.8	18.5	8.2
C1	25	150	901	1.4	4.9	9.6
D1	50	131	942	1.0	3.7	10.5

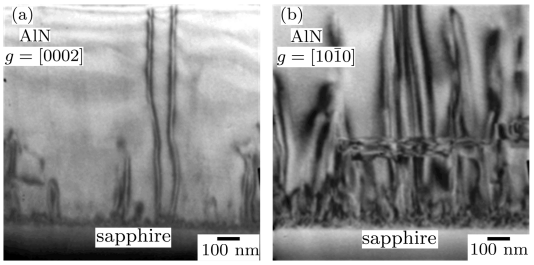


Fig. 3. Typical bright-field cross-sectional TEM images (sample C1) taken under different diffraction conditions with (a) $g = [0002]$, showing the screw TDs, and (b) $g = [10\bar{1}0]$, showing the edge TDs.

The 1×1 μm^2 AFM images of samples A2, B2, C2 and D2 are shown in Fig. 4. For all these nucleation-layer samples, islands can be observed on their surfaces. The surface RMS roughness, island dimensions and densities of these four nucleation samples are listed in Table 2. The diameters and heights of the islands on these samples increase with the nucleation thickness increasing. The island density also increases with the nucleation thickness increasing, except for sample A2 which has a thinnest nucleation but a highest island density of 1.85×10^{11} cm^{-2}.

By comparing the XRD and the AFM measurement results of the two sets of samples, it can be found that when the nucleation layer is thicker than a certain value (around 12.5 nm), the (102) XRD FWHM of AlN epi-layer increases with nucleation thickness increasing, whereas the (002) XRD FWHM shows an opposite trend. However, for sample A1 with a nucleation layer thinner than this value, although it has a very flat nucleation surface and narrow (002) XRD FWHM, the (102) XRD FWHM of 1197″ is the worst one.

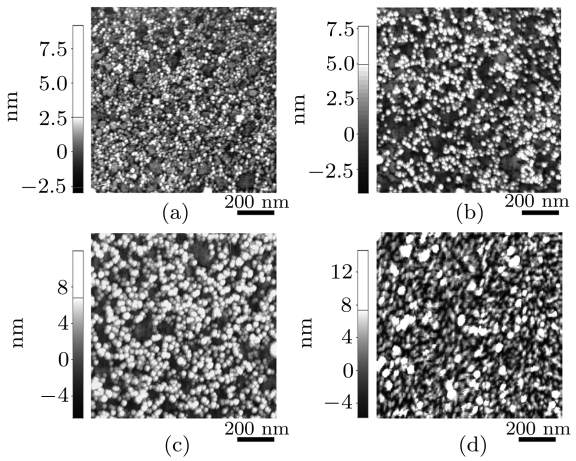


Fig. 4. AFM images of samples A2 (a), B2 (b), C2 (c) and D2 (d).

Table 2. Surface RMS roughness and nucleation island characteristics of nucleation-layer samples.

sample	1×1 μm^2 RMS roughness /nm	island diameter /nm	island height /nm	island density /$\times 10^{11}$ cm^{-2}
A2	0.94	20–30	0.7–2.5	1.85
B2	1.59	25–35	1.2–4	0.48
C2	2.61	30–40	3–6	0.70
D2	2.01	30–55	4–8	1.47

Since the lattice mismatch between AlN and sapphire substrate is as large as 13%, and the nucleation layer is grown under an N-rich condition with weak Al atom migration, small AlN islands tend to be formed at the beginning of nucleation. With the increase of nucleation thickness, these islands will grow larger in both vertical and lateral directions. Meanwhile, new islands may appear in flat regions. After nucleation, the AlN main layer will be grown directly based on these AlN islands, because of the absence of AlN decomposition or recrystallisation during the annealing process. Therefore, the quality and the density of the nucleation island both play crucial roles in the crystalline quality of AlN epi-layer, especially the tilts and rotations of nitride mosaic structures. During the initial growth of AlN main layer, because the Al adatom migration is enhanced by the Al-rich condition, the nucleation islands are considered to expand and coalesce laterally, but not to form new islands in flat regions. However, this will inevitably result in boundaries of crystal grains, which induce TDs in the epi-layer. Additionally, in a hexagonal AlN crystal, the Al–N bond along the *c*-direction is stronger than the three in-plane bonds.[17] Thus, during nucleation islands coalescing, there is a much higher possibility to induce rotations rather than tilts in mosaic structure model. In this sense, the higher nucleation island density will result in higher edge TD density, which is consistent with the AFM and (102) XRD measurement data. For (002) XRD results, larger nucleation islands may improve the quality of crystal grain, which is the possible reason why sample D1 has the narrowest (002) XRD FWHM. For sample A1, because the nucleation layer is too thin to complete the competition and the inosculation between initial islands, it has a very high nucleation island density, which results in the highest edge TD density. However, its nucleation surface is the smoothest one, which may be helpful to obtain a relatively narrow (002) XRD FWHM.

4. Conclusion

The effects of thickness of AlN nucleation grown at high temperature on AlN crystalline quality have been systematically investigated. It has been found that when nucleation layer is thicker than a certain value, the (102) XRD FWHM of AlN epi-layer increases with nucleation thickness increasing, whereas the (002) XRD FWHM shows an opposite trend. The mechanism is due to the fact that more crystal grains are formed with the increase of nucleation thickness, leading to more rotations of AlN mosaic structures, while larger nucleation crystal grains are favourable for the consistency of (0001) plane orientation, resulting in less tilt of the mosaic structures.

References

[1] Hirayama H, Yatabe T, Ohashi T and Kamata N 2008 *Phys. Status Solidi* C **5** 2283

[2] Dahal R, Al Tahtamouni T M, Lin J Y and Jiang H X 2007 *Appl. Phys. Lett.* **91** 243503

[3] Dabiran A M, Wowchak A M, Osinsky A, Xie J, Hertog B, Cui B, Look D C and Chow P P 2008 *Appl. Phys. Lett.* **93** 082111

[4] Sakai M, Ishikawa H, Egawa T, Jimbo T, Umeno M, Shibata T, Asai K, Sumiya S, Kuraoka Y, Tanaka M and Oda O 2002 *J. Cryst Growth* **244** 6

[5] Li X H Zhong F, Qiu K, Yin Z J and Ji C J 2008 *Chin. Phys.* B **17** 1360

[6] Chen X, Li S and Kang J 2008 *J. Mater. Sci.-Mater. Electron.* **19** S215

[7] Liu Q, Zhang R, Xie Z, Liu B, Xu F, Yao J, Nie C, Xiu X, Han P, Zheng Y and Gong H 2008 *Sci. China Ser.* E-*Tech. Sci.* **11** 1881

[8] Fälth J F, Davidsson S K, Liu X Y and Andersson T G 2005 *Appl. Phys. Lett.* **87** 161901

[9] Koblmueller G, Averbeck R, Geelhaar L, Riechert H, Hösler W and Pongratz P 2003 *J. Appl. Phys.* **93** 9591
[10] Edgar J H 1994 *Properties of Group-III Nitrides* (London: INSPEC, the Institution of Electrical Engineers) p4
[11] Wang H M, Zhang J P, Chen C Q, Fareed Q, Yang J W and Khan M A 2002 *Appl. Phys. Lett.* **81** 604
[12] Chierchia, R Böttcher T, Heinke H, Einfeldt S, Figge S and Hommel D 2003 *J. Appl. Phys.* **93** 8918
[13] Zheng X H, Chen H, Yan Z B, Han Y J, Yu H B, Li D S, Huang Q and Zhou J M 2003 *J. Cryst. Growth* **255** 63
[14] Paduano Q S, Weyburne D W, Serafinczuk J, Jasinski J and Liliental-Weber Z 2003 *Phys. Status Solidi* C 2014
[15] Srikant V, Speck J S and Clarke D R 1997 *J. Appl. Phys.* **82** 4286
[16] Lee S R, West A M, Allerman A A, Waldrip K E, Follstaedt D M, Provencio P P Koleske D D and Abernathy C R 2005 *Appl. Phys. Lett.* **86** 241904
[17] Edgar J H, Strite S, Akaski I, Amano H and Wetzell C 1999 *Properties, Processing and Applications of Gallium Nitride and Related* (London: INSPEC, the Institution of Electrical Engineers) p3